Title

DNA Damage Drives an Activin A–Dependent Induction of Cyclooxygenase-2 in Premalignant Cells and Lesions

Permalink

https://escholarship.org/uc/item/9f40r4n0

Journal

Cancer Prevention Research, 3(2)

ISSN

1940-6207

Authors

Fordyce, Colleen
Fessenden, Tim
Pickering, Curtis
et al.

Publication Date

2010-02-01

DOI

10.1158/1940-6207.capr-09-0229

Peer reviewed

DNA Damage Drives an Activin A–Dependent Induction of Cyclooxygenase-2 in Premalignant Cells and Lesions

Colleen Fordyce, Tim Fessenden, Curtis Pickering, Jason Jung, Veena Singla, Hal Berman, and Thea Tlsty

Abstract

Cyclooxygenase-2 (COX-2) catalyzes the rate-limiting step in the synthesis of prostaglandins. Its overexpression induces numerous tumor-promoting phenotypes and is associated with cancer metastasis and poor clinical outcome. Although COX-2 inhibitors are promising chemotherapeutic and chemopreventative agents for cancer, the risk of significant cardiovascular and gastrointestinal complications currently outweighs their potential benefits. Systemic complications of COX-2 inhibition could be avoided by specifically decreasing COX-2 expression in epithelial cells. To that end, we have investigated the signal transduction pathway regulating the COX-2 expression in response to DNA damage in breast epithelial cells. In variant human mammary epithelial cells that have silenced p16 (vHMEC), double-strand DNA damage or telomere malfunction results in a p53- and activin A–dependent induction of COX-2 and continued proliferation. In contrast, telomere malfunction in HMEC with an intact p16/Rb pathway induces cell cycle arrest. Importantly, in ductal carcinoma *in situ* lesions, high COX-2 expression is associated with high γH2AX, TRF2, activin A, and telomere malfunction. These data show that DNA damage and telomere malfunction can have both cell-autonomous and cell-nonautonomous consequences and can provide a novel mechanism for the propagation of tumorigenesis. *Cancer Prev Res; 3(2); 190–201. ©2010 AACR.*

Introduction

Cyclooxygenase-2 (COX-2) is one of two enzymes that catalyze the rate-limiting step in the synthesis of prostaglandins. In contrast to the widespread constitutive expression of COX-1, COX-2 is strongly inducible by a variety of agents in a limited number of cell types, including neoplastic tissues (1, 2). Through the production of prostaglandins, COX-2 plays a significant role in cancer by increasing proliferation, motility, invasion, angiogenesis, and resistance to apoptosis, while also repressing host immune response to tumors (3–6). COX-2 has a profound effect on every aspect of breast cancer including initiation, progression to invasive disease, and finally, metastasis. For example, high COX-2 in benign atypical hyperplasia lesions is associated with the increased risk of developing breast cancer (7). COX-2 is associated with mammographic density, a significant risk factor for breast cancer (8). In combination with p16/Rb pathway malfunction, high COX-2 expression predicts progression of preinvasive ductal carcinoma

in situ (DCIS) lesions to invasive ductal carcinoma (IDC; ref. 9). COX-2 enhances breast cancer metastasis to bone in mouse models (10) and is associated with bone marrow and brain metastasis (11, 12). Consequently, high COX-2 expression is associated with poor prognosis in both DCIS and IDC (9, 13, 14).

COX-2 is an ideal target for chemopreventatives and chemotherapeutics. Nonselective COX-2 inhibitors (nonsteroidal anti-inflammatory drugs), such as aspirin, and COX-2–specific inhibitors (coxibs) decrease cancer mortality, recurrence, and incidence (15–18). However, the use of these drugs is associated with gastrointestinal and cardiovascular complications (1, 19). One plausible explanation for these side effects is the eicosanid imbalance theory, i.e., the inhibition of COX-2 in the vasculature decreases the vasodilator PGI2, without reducing COX-1–dependent vasoconstrictive thromboxanes (1, 19). Decreasing COX-2 expression in a single cell type might mitigate these side effects; for instance, loss of COX-2 in breast epithelial cells could reduce breast cancer incidence and progression without inducing the complications associated with nonsteroidal anti-inflammatory drugs or coxibs. Such an approach requires a detailed understanding of the cell type–specific mechanisms that govern COX-2 expression. We have identified a subpopulation of epithelial cells within the human breast that upregulates COX-2, an event that coincides with increased genomic instability, telomere malfunction (3, 20), and accumulation of the telomere-binding protein, TRF2. Here, we identify the upstream pathways responsible for this COX-2 induction and unmask novel biology that has cell-autonomous as

Authors' Affiliation: Department of Pathology, University of California, San Francisco, San Francisco, California

Corresponding Author: Thea Tlsty, Department of Pathology, University of California, San Francisco, 513 Parnassus Avenue, HSW 501, San Francisco, CA 94143. Phone: 415-502-6115; Fax: 415-502-6163; E-mail: thea.tlsty@ucsf.edu.

American Association for **Cancer Research**

well as cell-nonautonomous repercussions for tumor progression.

Materials and Methods

Cell culture

HMEC were isolated from disease-free breast tissue of nine individuals (CM7, RM9, RM15, RM16, RM18, RM40, RM45, RM46, and RM146). Epithelial cells were propagated as described in ref. (20). Activin A and the p38 inhibitor, SB203580 (Sigma), were added to culture medium for 48 and 24 h, respectively, before harvest at the doses shown in Figs. 2 and 4. Etoposide and NU7026 (Sigma) were added to the culture medium for the times indicated in Figs. 1 and 3. The medium was removed before exposure to UVC and was immediately replaced.

Expression of TRF2, hTERT, and short hairpins

The *TRF2* gene, provided by Dr. T. De Lange (Rockefeller University, New York, NY), was inserted into the pWP1 lentiviral expression vector obtained from Dr. D. Trono (Swiss Federal Institute of Technology, Lausanne, Switzerland). The pWP1-hTERT construct was provided by Dr. E. Blackburn (University of California, San Francisco, San Francisco, CA). The pWP1-TRF2 and pWP1-hTERT constructs were packaged in 293T cells. Infection efficiency was monitored using green fluorescent protein expression driven by an IRES sequence. The control luciferase short hairpin (pGL3) and the pLKO vector were provided by Dr. M. McManus (University of California, San Francisco, CA). The activin A short hairpin (5′-GAACTGTTGCTCTCT-GAAA-3′) was designed using PSICO Oligo Maker. ATM and p53 short hairpins were published previously (21, 22). Infected cells were maintained in 2 μg/mL puromycin (Sigma).

Wound closure assay

Wound closure assays were performed as described in ref. (23).

Quantitative PCR

Quantitative PCR was done using standard methods. Primer-probe sets for COX-2 (Hs00153133), TRF2 (Hs00194619), hTERT (Hs00162669), activin A/inhibin A (Hs00170103), ATM (HS00175892), p53 (Hs99999147), and p21 (Hs00355782) were obtained from ABI. Glucoronidase B (IDT) expression was used to normalize for variances in input cDNA.

Microarray analysis

RNA was purified (RNeasy, Qiagen) and amplified using the MessageAmp II-Biotin kit (Ambion). Amplified RNA was labeled using the enzo BioArray High Yield RNA transcript labeling kit (Affymetrix). Microarray hybridization and analysis were done at the J. David Gladstone Institutes Core Genomics Laboratory.

Western blotting and ELISA

Western blots were done as described in ref. (4). Activin A protein and prostaglandin levels were measured using the Duo-Set Activin ELISA kit (R&D Systems) and the Prostaglandin E$_2$ E1A Elisa kit (Cayman).

Tissue samples

High-grade (n = 7) and low-grade (n = 8) nonrecurrent DCIS specimens were obtained with institutional review board approval from the Helen Diller Comprehensive Cancer Tissue Core (University of California, San Francisco). Patients were identified through anonymous reference numbers in accordance with federal guidelines.

Telomere PNA hybridization

Chromosome spreads were prepared, processed, and analyzed as described in ref. (20). An average of 75 nuclei each were evaluated for parent, pWP, and TRF2-vHMEC and hTERT-vHMEC.

Tissue preparation and immunohistochemistry

Five-micrometer sections were cut from paraffin-embedded tissue blocks adjacent to sections used for telomere DNA content determination. Immunohistochemistry was performed using standard protocols. Microwave antigen retrieval was accomplished using 0.001 mol/L EDTA (pH = 8) for COX-2; Antigen Unmasking Solution (Vector Laboratories) was used for TRF2; and 0.01 mol/L citrate buffer (pH = 6.0) was used for activin A and γH2AX. Antibodies against COX-2 (1:200; DAKO), TRF2 (1:20; Imgenex), γH2AX (1:150; Upstate), and activin A (1:100; AbD Serotech) were used. A blocking step (0.01% Triton-X 100 in PBS for 1 h) was done before the addition of the TRF2 antibody. Evaluation of γH2AX, TRF2, COX-2, or activin A staining intensity was done in a blinded fashion. For COX-2 and activin A, staining intensity was scored as low to absent (low) or moderate to strong (high). The number of γH2AX- or TRF2-positive nuclei were counted in at least 500 cells and expressed as a percentage of the total number of nuclei per DCIS lesion. The mean number of γH2AX-positive (28%) or TRF2 (29%)-positive nuclei was used to divide the lesions into high- or low-expression groups.

Telomere DNA content determination

For each case, a 5-μm tissue section was stained with H&E, and cellular morphology was evaluated and used to guide microdissection of 6 × 25 μm serial sections. Telomere content was determined as described previously (24).

Statistical methods

Two-sided t tests assuming unequal variance were used to test the relationships between gene expression or activin A protein or prostaglandin levels in cells overexpressing vector, TRF2, or hTERT, or exposed to drugs, and the relationship between telomere DNA content and γH2AX, TRF2, activin A, and COX-2. χ^2 test was used to evaluate

the relationship between staining intensity (high or low) for γH2AX, TRF2, and activin A or COX-2. The Jmp 7.0 statistical package (SAS Institute) was used for all analyses.

Results

Double-strand DNA damage, in contrast to single-strand DNA damage, is a potent inducer of COX-2 in mammary epithelial cells with a compromised p16/Rb pathway

Several types of DNA damage induce COX-2 (3, 4) in variant human mammary epithelial cells with a compromised p16/Rb pathway (vHMEC). To more fully elucidate

these observations, we exposed vHMEC to agents that induce double-strand (etoposide) or single-strand (UVC) DNA breaks. Treatment of vHMEC with etoposide (0, 10, and 100 μmol) and UVC (0, 30, 60, and 120 J/m^2) induced a cell death of ~5.6% (100 μmol etoposide) and 3.5% (60 J/m^2 of UVC), respectively, after 24 hours. COX-2 mRNA levels, measured by quantitative PCR, were greater in cells treated with 10 and 100 μmol etoposide (3.1- and 4.6-fold; $P = 0.009$ and $P = 0.0005$, respectively) compared with controls and exhibited a sustained induction. In contrast, exposure to 60 or 120 J/m^2 UVC decreased COX-2 mRNA levels 3.7- and 3.6-fold compared with controls ($P = 0.0006$ and $P = 0.0006$, respectively)
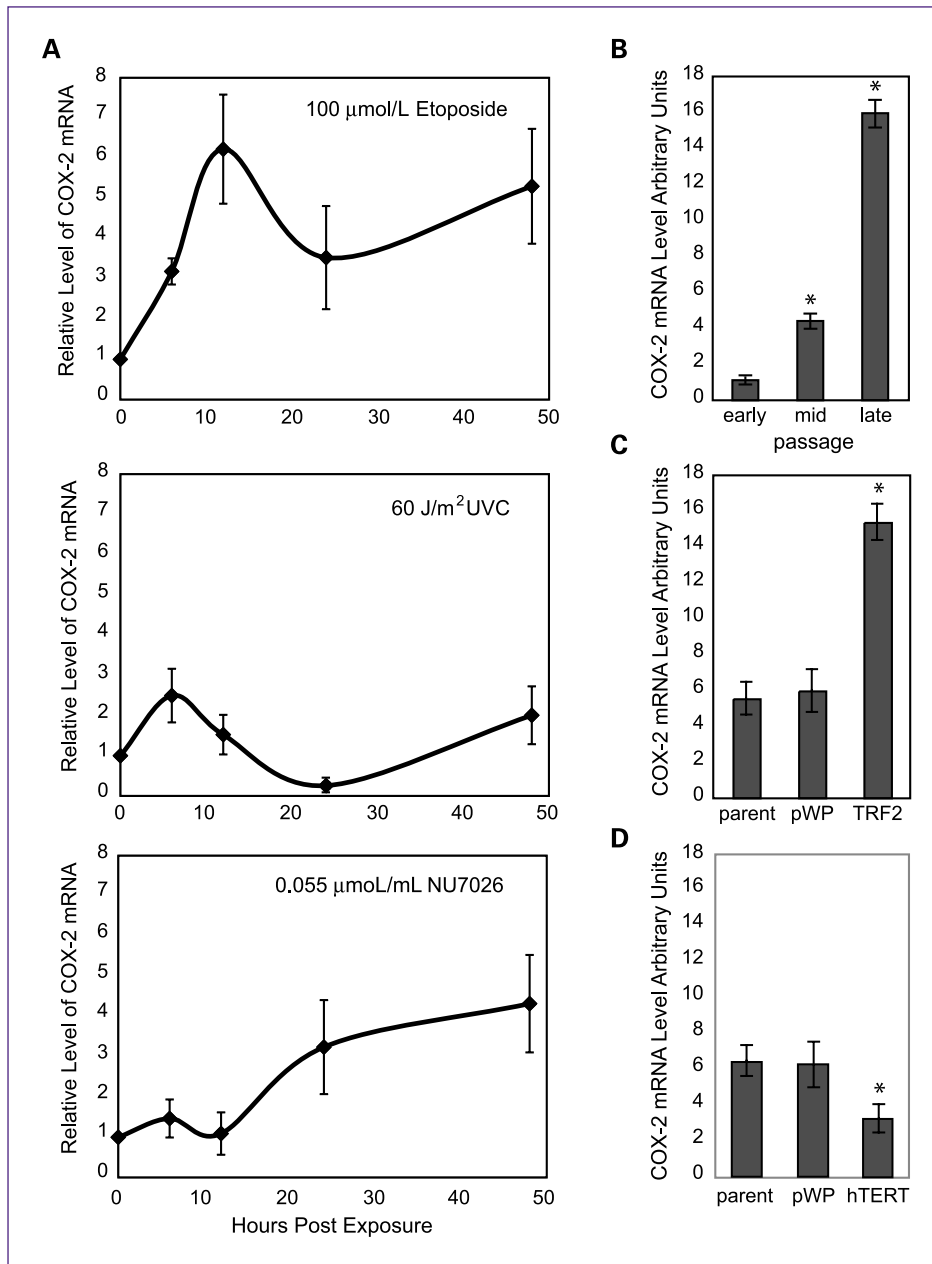
Fig. 1. DNA damage induces COX-2 in vHMEC. RM9, RM15, and RM16 were used in A to C. A, vHMEC were exposed to 100 μmol/L etoposide (*top*), 60 J/m^2 UVC (middle), and 0.055 μmol/mL NU7026 (bottom), and mean COX-2 mRNA levels were measured at the indicated times. Points, mean; bars, SEM. B, COX-2 mRNA levels in early-, mid-, or late-passage vHMEC. C, COX-2 mRNA levels in vHMEC infected with lentivirus containing either *TRF2* or empty vector (pWP1). D, COX-2 mRNA levels in vHMEC (RM15, RM16, and RM18) infected with lentivirus containing either *hTERT* or empty vector (pWP1). *, statistically significant ($P < 0.05$) changes in expression compared with vector or untreated control.
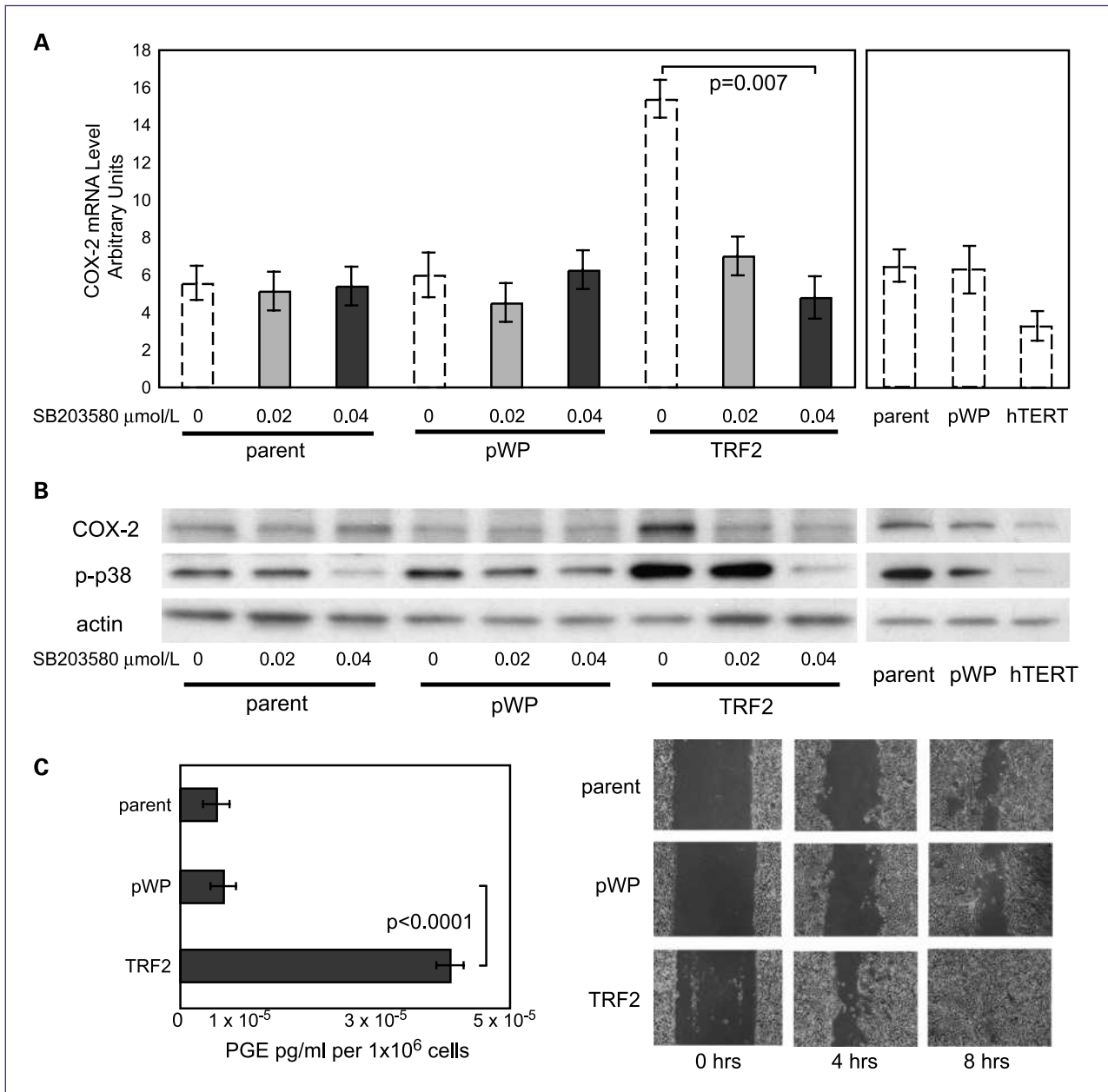
Cancer Prevention Research

Fig. 2. TRF2 induces COX-2 through a phospho-p38–dependent mechanism. A, mean COX-2 mRNA levels in untreated parent vHMEC, pWP1, TRF2-vHMEC, or hTERT-vHMEC (hatched columns, shown in Fig. 1C) or treated with the phospho-p38 inhibitor SB203580 for 24 h (gray columns). B, representative immunoblot showing COX-2, phospho-p38 (*p-p38*), and actin (loading control) protein levels for the conditions described in A. C, mean levels of prostaglandins in conditioned medium (left). Wounding assay for parent, pWP, or TRF2-vHMEC (right).

after 24 hours. We then compared the kinetics of COX-2 induction in vHMEC exposed to 100 μmol etoposide or 60 J/m^2 of UVC for 6, 12, 24, and 48 hours (selected treatment conditions were based on the similar cytotoxicity and significant changes in COX-2 mRNA levels described above). Exposure to both treatments resulted in a biphasic induction of COX-2 mRNA; expression peaked at 6 to 12 hours and 48 hours (Fig. 1A). However, the magnitude of induction was lower and of shorter duration following

exposure to UVC compared with etoposide, suggesting that double-strand DNA (dsDNA) breaks are more potent and sustained inducers of COX-2 in vHMEC than single-strand DNA breaks.

Endogenously induced dsDNA damage, through telomere malfunction, induces COX-2

As vHMEC proliferate, they lose telomeric DNA, accumulate genomic instability, and upregulate COX-2

(3, 20). We hypothesized that telomere malfunction, a type of dsDNA damage, which occurs early and nearly universally in epithelial cancers, might also induce COX-2. Based on a report showing that inhibition of DNA-PK kinase activity by NU7026 resulted in telomere malfunction (25), we tested the effect of this treatment (0.055 μmol/mL NU7026) on COX-2 expression in vHMEC. We observed a 10.8% cell death and a 3.2-fold increase in COX-2 mRNA 24 hours after exposure (Fig. 1A). Subsequent kinetic experiments showed that treatment with NU7026 also resulted in a biphasic induction of COX-2 mRNA with peak expression at 6 hours (1.5-fold) and 48 hours (4.32-fold).

To directly assess if telomere malfunction induced COX-2 in vHMEC, we modulated telomere function by overexpressing two telomere-binding proteins: TRF2 and hTERT (Supplementary Fig. S1). TRF2 is a negative regulator of telomere length (26–29), whereas hTERT is the reverse transcriptase that lengthens telomeres (Supplementary Fig. S1). Consistent with previous reports, TRF2 overexpression, to levels observed in cancer cell lines and tissues, induced telomere malfunction and a >6-fold increase in abnormal metaphase spreads including duplications, deletions, translocations, and chromosome breaks ($P < 0.0001$). Cells exhibited a concomitant accumulation of the DNA damage protein γH2AX. In stark contrast, hTERT, when expressed in these cells, maintained telomere function (Supplementary Fig. S2) and failed to induce significant chromosomal abnormalities. Mean COX-2 mRNA and protein levels increased
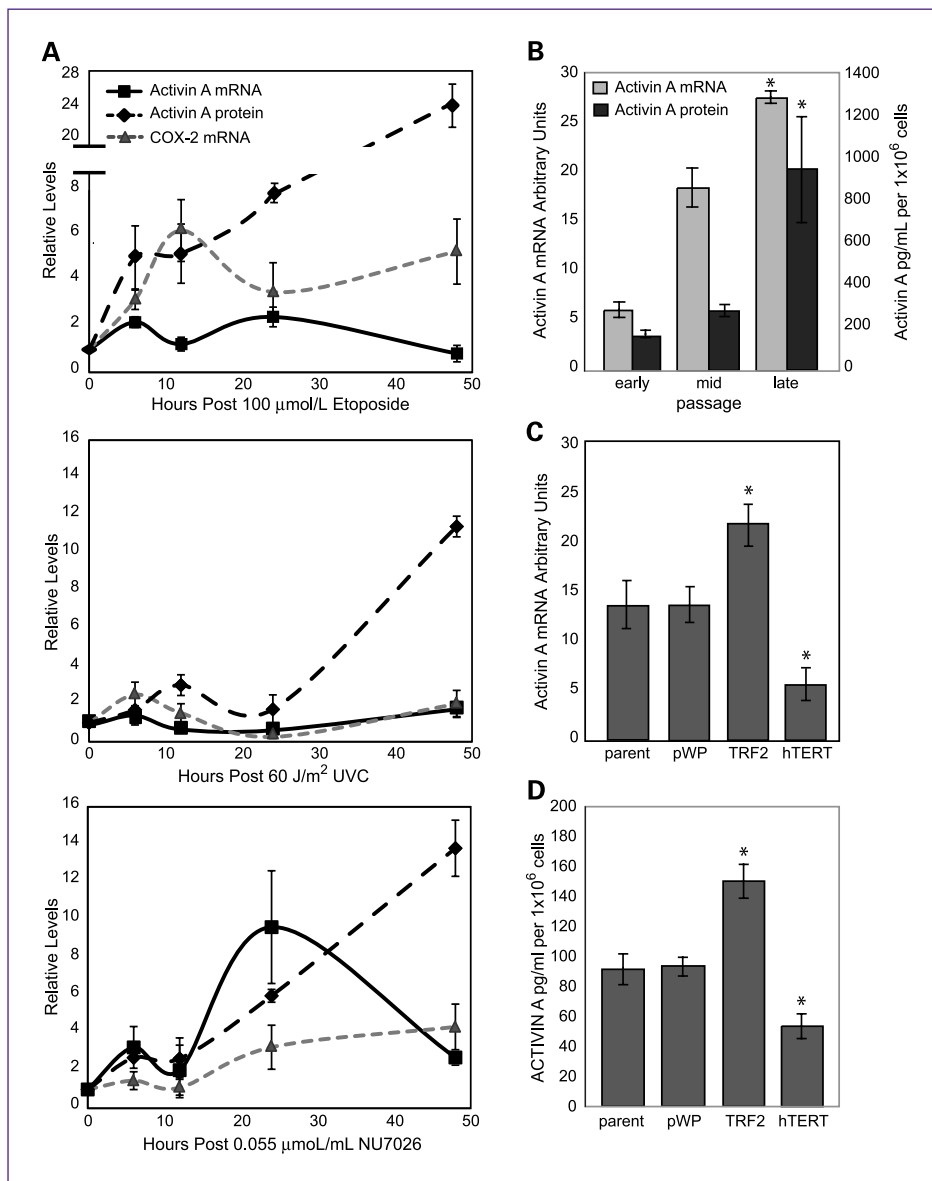

Fig. 3. Activin A is induced by DNA damage and coincides with COX-2 expression. A, vHMEC (RM9, RM15, and RM16) were treated as described in Fig. 1A. Line graphs, the relative level of COX-2 and activin A mRNAs and activin A protein in conditioned medium compared with the untreated control. COX-2 mRNA levels (shown in Fig. 1A) are indicated for comparison (light gray dashed line). B, mean activin A mRNA levels (light gray columns) in vHMEC (RM9, RM15, and RM16) and protein levels (dark gray columns) in early-, mid-, and late-passage RM9 vHMEC in duplicate experiments. Activin A mRNA (C) and protein (D) levels in RM9, RM15, RM16, and RM18 vHMEC overexpressing TRF2, hTERT, or vector (pWP) or mock-infected (parent). *, $P < 0.05$.

Fig. 4. Activin A and p53 are necessary for COX-2 induction. A, activin A levels were reduced using shRNA. Mean relative COX-2 and activin A mRNA and activin A protein levels measured as described in Fig. 3B in RM9, RM15, and RM16 and expressed relative to parent (parent, pWP1, or TRF2) or pGL3 (all others). B, COX-2 mRNA levels in vHMEC incubated with exogenous activin A (left). Immunoblot showing COX-2, phospho-p38 (*p-p38*), and actin (loading control) protein levels for each treatment. Conditioned medium from parent, vector, or TRF2-vHMEC obtained from two donors (RM9 and RM15) was diluted 1:1 and added to vHMEC obtained from three donors (RM9, RM15, and RM16). Corresponding immunoblots of treated cells showing COX-2, phospho-p38, and actin (loading control) expression (*right*). C, ATM and p53 levels were reduced using shRNA. Mean COX-2 and activin A mRNA and activin A protein levels in RM9, RM15, and RM16 were expressed relative to parent (parent, pWP1, or TRF2) or pGL3 (all others). *, statistically significant changes compared with either parent, pGL3, or TRF2+pGL3 (A and C). *, $P < 0.05$.
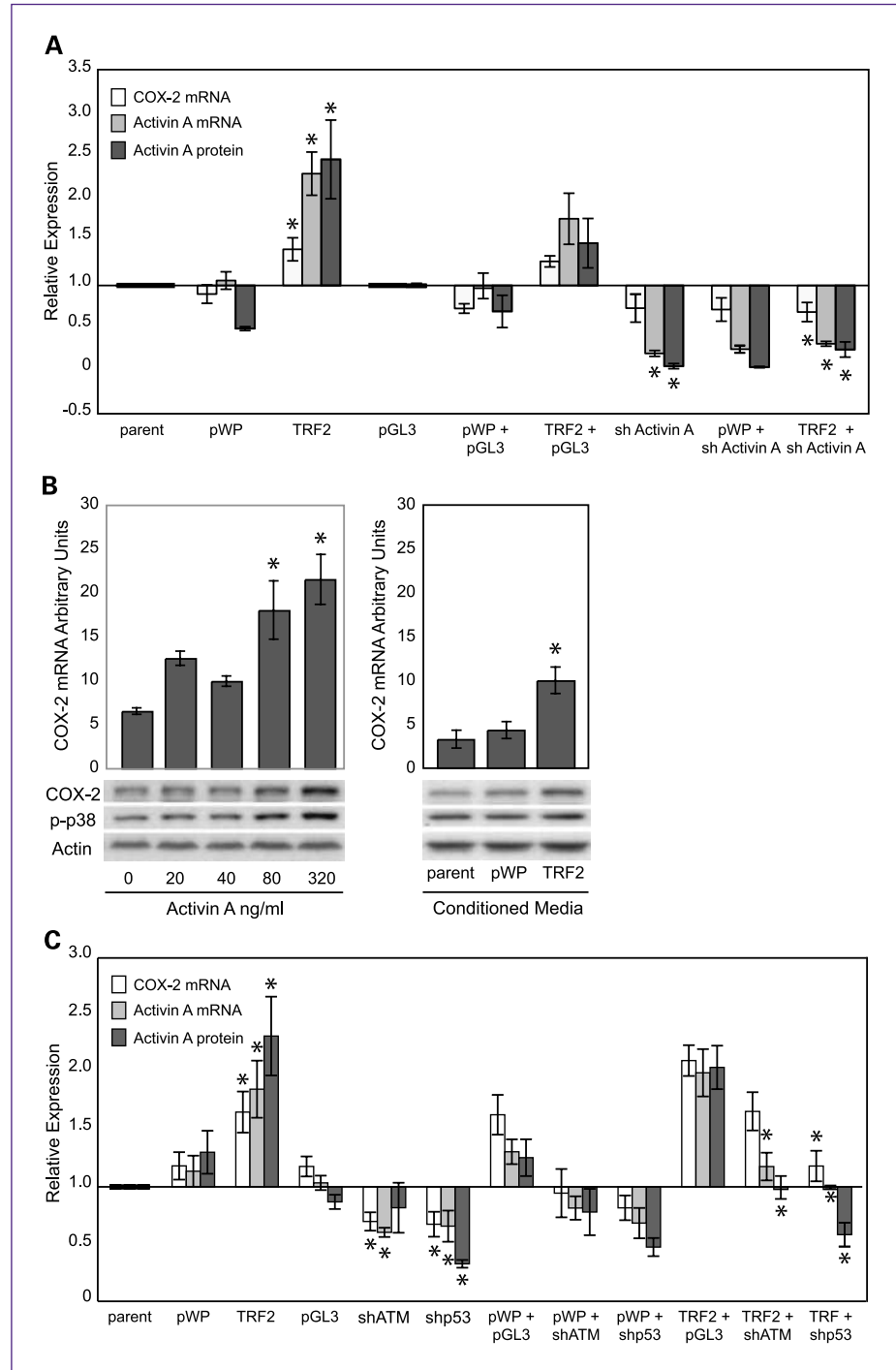
~3-fold in vHMEC overexpressing TRF2 (TRF2-vHMEC) compared with vector ($P = 0.01$; Figs. 1C and 2B). In contrast, COX-2 mRNA and protein levels were significantly downregulated (3.2 units, $P = 0.02$) in vHMEC overexpressing hTERT (hTERT-vHMEC; Figs. 1D and 2B). Thus, proteins that affect telomere function modulate COX-2 expression.

COX-2 overexpression resulting from TRF2-induced telomere malfunction alters cellular phenotypes

Next, we determined if TRF2-vHMEC displayed alterations of known COX-2–dependent phenotypes, i.e., production of prostaglandins and cell motility. Mean levels of prostaglandins increased ~6-fold in TRF2-vHMEC compared with vector ($P < 0.0001$; Fig. 2C), illustrating that

even a moderate COX-2 overexpression can result in dramatic downstream events. Cell-wounding assays revealed that TRF2-vHMEC were more motile, filling a "wound" in 8 hours, whereas parent and vector required 12 hours (Fig. 2C). Thus, increased COX-2 expression in TRF2-vHMEC alters cellular phenotypes.

Upregulation of COX-2 induced by TRF2 is phospho-p38 dependent

Phosphorylation of p38 is necessary for COX-2 mRNA stabilization and, consequently, for increased protein levels in late-passage vHMEC (3, 4). Phospho-p38 was upregulated in TRF2-vHMEC and repressed in hTERT-vHMEC (Fig. 2B). To determine if phospho-p38 was necessary for COX-2 induction in response to TRF2, we exposed early-passage parent, vector, and TRF2-vHMEC to the phospho-p38 inhibitor SB203580. Exposure to 0.02 or 0.04 μmol/L SB203580 reduced mean COX-2 mRNA levels by 49% and 71% ($P = 0.007$), respectively, in TRF2-vHMEC. Correspondingly, COX-2 and phospho-p38 protein levels were decreased following exposure to SB203580, showing that phospho-p38 was indeed necessary for TRF2 to induce COX-2 in vHMEC.

Telomere malfunction induces activin A

Gene expression profiling analysis for genes showing at least a 1.4-fold expression change in TRF2-vHMEC compared with vector (Supplementary Table S1) enabled us to identify candidate molecules upstream of p38 in TRF2-vHMEC. Among the upregulated genes was an attractive candidate, activin A. Activin A is a secreted member of the transforming growth factor-β (TGF-β) superfamily and can promote p38 phosphorylation (30, 31). Quantitative PCR validated the upregulation of activin A mRNA in TRF2-vHMEC and its downregulation in hTERT-vHMEC compared with vector control (Fig. 3C). Consistent with this, activin A protein is elevated in conditioned medium from TRF2-vHMEC and is reduced in conditioned medium from hTERT-vHMEC compared with control ($P = 0.007$ and $P = 0.01$, respectively).

Because telomere function can be impaired by the progressive loss of telomere DNA during cellular replication, we predicted that activin A would increase during continued propagation of vHMEC. We found that activin A protein and mRNA levels increased 4- to 5-fold in late versus early-passage vHMEC (Fig. 3B). Similarly, treatment with NU7026, which induces telomere malfunction, increased activin A mRNA and protein levels (Fig. 3A).

We then asked if DNA damage caused by etoposide or UVC could also induce activin A. Activin A mRNA and protein were significantly upregulated in vHMEC exposed to either agent (Fig. 3A). However, activin A levels were greater in vHMEC treated with etoposide or NU7026 than with UVC. As observed for COX-2, activin A mRNA and protein induction was biphasic and peaked at similar

intervals. Collectively, these data showed that activin A mRNA and protein were preferentially induced by dsDNA damage and coincided with the expression of COX-2.

Activin A is necessary and sufficient for COX-2 induction

Next, we assessed whether activin A was necessary for COX-2 induction. TRF2-vHMEC, parent, and vector were infected with lentivirus expressing either a control short hairpin RNA (shRNA) against luciferase (pGL3) or a shRNA against activin A to reduce its expression. Basal activin A mRNA and protein levels were reduced by 79% and 75% ($P < 0.001$ and $P < 0.0001$), respectively, compared with control shRNA (Fig. 4A). Activin A shRNA reduced basal COX-2 mRNA in vHMEC by 27%, but was not statistically significant (Fig. 4A). In contrast, mean COX-2 mRNA levels decreased 46% in TRF2-vHMEC expressing activin A shRNA compared with TRF2-vHMEC expressing pGL3 ($P = 0.002$). We then investigated whether activin A was sufficient to induce COX-2 by exposing vHMEC to exogenous activin A or to conditioned medium from either TRF2-vHMEC or controls. At the two highest doses of activin A (30, 32), mean levels of COX-2 mRNA were increased ~3-fold ($P = 0.04$ and $P = 0.01$, respectively; Fig. 4B). Likewise, vHMEC propagated in conditioned medium from TRF2-vHMEC had increased COX-2 mRNA ($P = 0.008$) and protein (Fig. 4B) compared with vHMEC propagated in conditioned medium from vector. COX-2 and phospho-p38 protein levels were also increased by both treatments (Fig. 3B). Thus, activin A is both necessary and sufficient for COX-2 expression, showing that secreted activin A can act in a cell-nonautonomous fashion to induce COX-2 in absence of DNA damage.

The dsDNA damage response effectors ATM and p53 are necessary for COX-2 induction

ATM and p53 are two essential members of the dsDNA damage response. Importantly, p53 is necessary for COX-2 induction (33). Using shRNAs, we repressed ATM and p53 expression by 68% and 93%, respectively, in control and in TRF2-vHMEC (Supplementary Fig. S3). ATM or p53 silencing decreased basal levels of COX-2 mRNA, activin A mRNA, and activin protein in vHMEC by 40%, 41%, and 53%, and 42%, 36%, and 61%, respectively, compared with control shRNA (Fig. 4C). Similarly, repression of ATM and p53 in TRF2-vHMEC decreased COX-2 mRNA, activin A mRNA, and activin protein by 16.5%, 41%, and 48%, and 43%, 51%, and 71%, respectively, compared with TRF2-vHMEC expressing a control shRNA (pGL3).

COX-2 is induced by DNA damage in p16-competent HMEC

Previously, we reported that exogenous expression of COX-2 in HMEC, with an intact p16/pRb pathway, results in cell cycle arrest and induction of p16 and p21 (9), implying that HMEC and vHMEC might

Fig. 5. DNA damage induces activin A, COX-2, and growth arrest in p16-competent HMEC. A, HMEC were exposed to 100 μmol/L etoposide (RM40, RM45, and RM46) or to 60 J/m² of UVC (RM45) as described in Fig. 1A. Line graphs, relative COX-2 and activin A mRNA levels and activin A protein levels in conditioned medium compared with the untreated control. B, activin A, COX-2, p16, and p21 mRNA levels in parent, vector (pWP1) or TRF2-HMEC (CM7 and RM146). *, P < 0.05. C, population doublings in HMEC (CM7) infected with lentivirus containing TRF2 or empty vector (pWP1) or parent HMEC. D, overview of the DNA damage–dependent COX-2 induction and its consequences in HMEC (intact p16/Rb) or vHMEC (silenced p16).
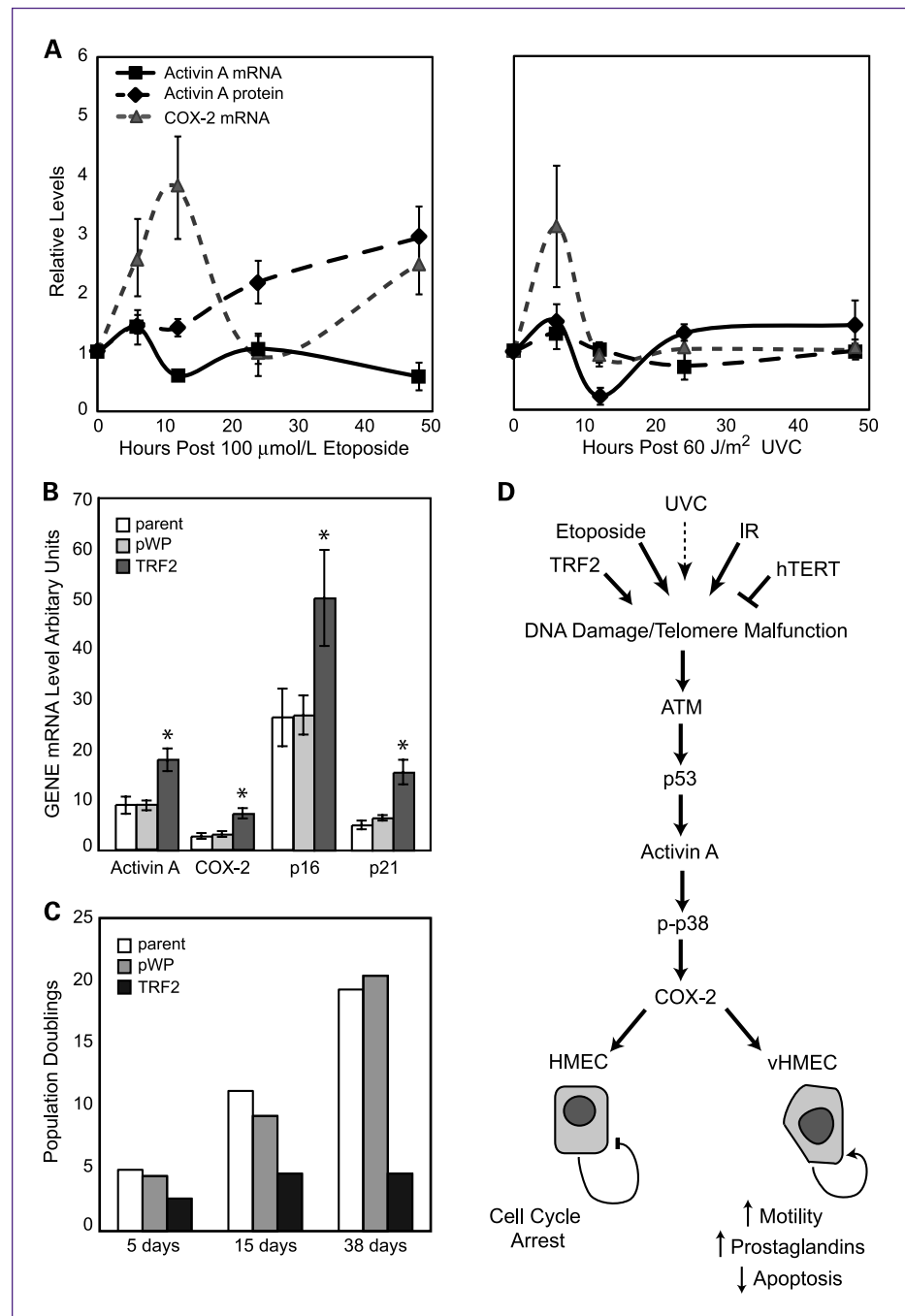
respond differently to DNA damage. Upon treatment of HMEC with etoposide or UVC, COX-2 mRNA, activin A mRNA, and activin A protein were induced, although at a lower level than in vHMEC. Consistent with our observations in vHMEC, HMEC treated with etoposide exhibited a biphasic induction of COX-2 and activin A with peaks at 6 to 12 hours and 48 hours. Exposure to UVC induced COX-2 and activin A, both of whose expression peaked at 6 hours, but in contrast to treatment with etoposide,

then returned to basal levels after 24 hours (Fig. 5A). Thus, COX-2 is induced by DNA damage in HMEC with an intact p16/Rb pathway.

COX-2 overexpression in p16-competent HMEC is growth suppressive

We then examined how HMEC (p16 competent) would respond to sustained DNA damage induced by TRF2 overexpression. When compared with vector,

TRF2-HMEC had a statistically significant increase in COX-2 ($P = 0.006$) and activin A ($P = 0.005$) mRNAs (Fig. 5B). However, TRF2-HMEC also upregulated p16 and p21 (Fig. 5B), displayed flattened vacuolated morphology, entered growth arrest (Fig. 5C), and exhibited a decreased fraction of cells in S phase (Supplementary Fig. S4), all phenotypes consistent with senescence. Thus, in the context of an intact p16/Rb pathway, DNA damage results in increased activin A and COX-2, but also in induction of growth arrest. These data show that in contrast to vHMEC, the cellular response to COX-2 in HMEC is both self-limiting and growth suppressive.

COX-2 expression in DCIS is associated with manifestations of a dsDNA damage response and increased TRF2 and activin A expression

COX-2 is often upregulated in DCIS (34) where it has prognostic significance (9, 13). Additionally, DCIS is the earliest stage in breast cancer at which loss of telomere DNA can be widely detected (35). We used a pilot cohort of 15 DCIS cases to determine whether changes in telomere content, a proxy for telomere length (24), were associated with alterations in γH2AX, TRF2, activin A, and COX-2 expression. DCIS lesions were microdissected to produce enriched populations of tumor cells that were used for DNA purification. Telomere content
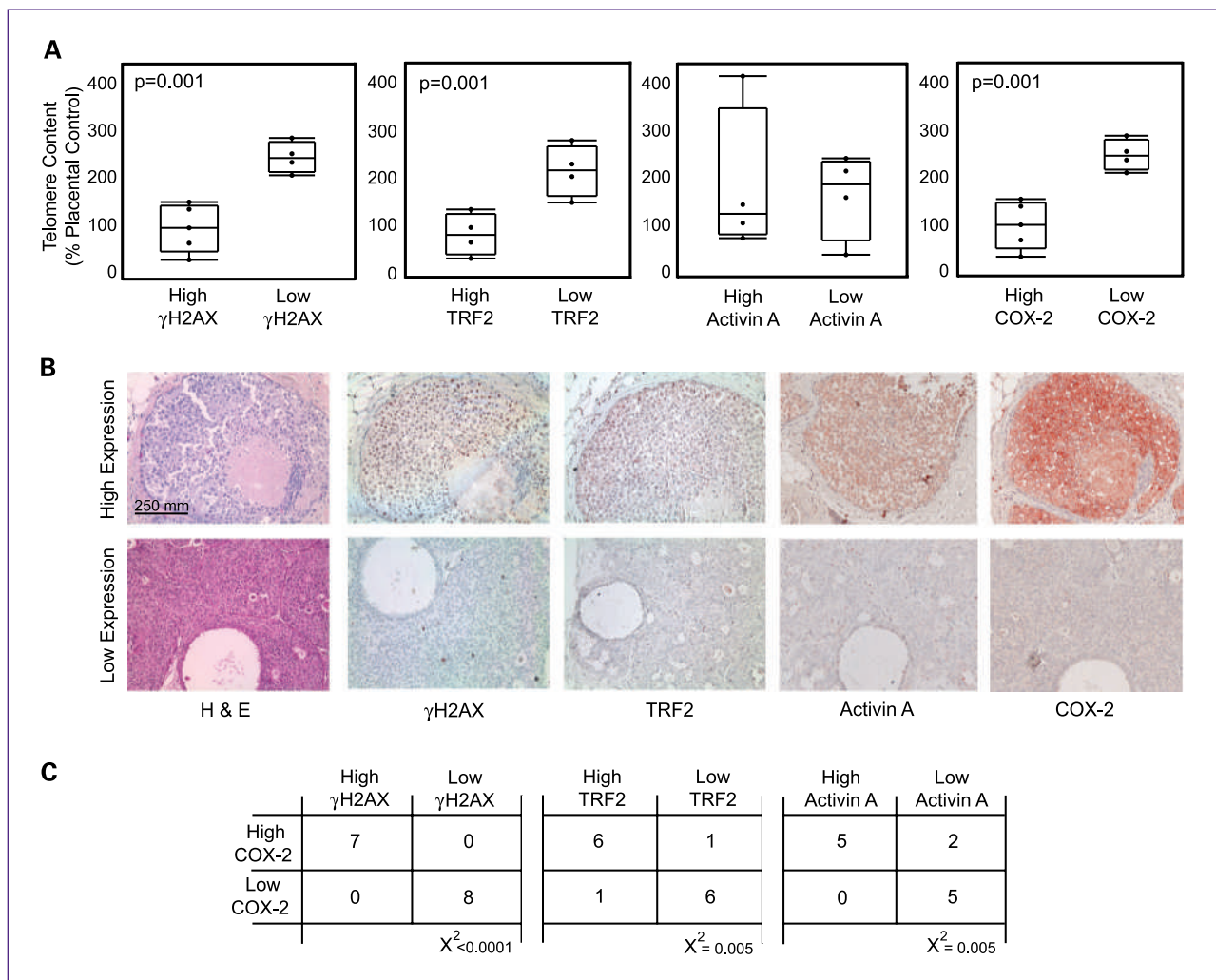

Fig. 6. Telomere content is inversely associated with TRF2, activin A, and COX-2 expression in DCIS. A, γH2AX, TRF2, activin A, and COX-2 protein levels were evaluated by immunohistochemistry. Lesions were divided into two groups based on staining intensity for each protein. Telomere content in DCIS lesions was expressed as a percentage of placental DNA. Box plots show the relationship between γH2AX (far left), TRF2 (left), activin (right), and COX-2 (far right) and telomere content in high- and low-expression lesions. Inset, P values for each comparison. B, examples of serial sections for high- and low- expression DCIS lesions (×20) stained with H&E, and γH2AX, TRF2, activin A, and COX-2 antibodies. Nuclei counterstained with hematoxylin (blue) and primary antibodies against each antigen detected using AEC (red). C, contingency tables showing the number of cases with high or low COX-2 levels versus the number of cases with high or low γH2AX, TRF2, and activin A.

was measured in 9 of the 15 lesions from which sufficient DNA was obtained.

Expression levels of γH2AX, TRF2, activin A, and COX-2 were evaluated by immunohistochemistry in serial sections of the 15 DCIS cases (Supplementary Table S2) and were used to divide lesions into two groups (see Materials and Methods). DCIS lesions with high γH2AX, TRF2, or COX-2 expression had lower telomere content than those with low γH2AX, TRF2, or COX-2 expression ($P = 0.001$, $P = 0.001$, $P = 0.001$, respectively). Although not statistically significant, mean telomere content was reduced in three of the four lesions with high activin A (Fig. 6). Moreover, COX-2 expression levels were correlated with those of γH2AX ($\chi^2 = 0.005$), TRF2 ($\chi^2 = 0.005$), and activin A ($\chi^2 < 0.0001$). Thus, our findings *in vitro* are recapitulated *in vivo*: DNA damage induced by telomere malfunction and characterized by low telomere content, high γH2AX, and high TRF2 expression, is associated with increased activin A and COX-2 expression.

Discussion

Here, we show for the first time that dsDNA damage and telomere malfunction in human breast epithelial cells results in a p53- and activin A–dependent COX-2 induction. By identifying signaling events leading to COX-2 induction, this study complements our previous work establishing a direct link between COX-2 and malignant phenotypes (3). Strikingly, COX-2 expression, and its associated phenotypes, are not confined to the initial cell with telomere malfunction, but are also induced in cells in the absence of DNA damage through the cell-nonautonomous action of activin A (Fig. 5D). Although induction of this pathway is self-limiting (i.e., leading to cell cycle arrest) in HMEC (intact p16/Rb pathway), it is not in vHMEC (silenced p16), where cells continue to proliferate. Finally, we show *in vivo* that high COX-2 expression is associated with high levels of γH2AX, TRF2, and activin A in a pilot cohort of DCIS lesions.

Our study highlights the coordinated action of p53, activin A, and p38 in inducing COX-2 following dsDNA damage. To our knowledge, this is the first report of an activin A–dependent COX-2 induction in human cells. A similar observation has been reported in rat macrophages (36). Multiple stimuli can induce COX-2 including mitogens, cytokines, hormones, irradiation, oncogene activation, and inflammation (33, 37). Many of these factors induce p53, which can in turn increase COX-2 expression. Interestingly, COX-2 induction decreases p53-dependent apoptosis in vHMEC, suggesting that COX-2 represses p53 function (38). This feedback loop may explain the biphasic activin A and COX-2 induction in response to DNA damage described here.

Activin A is a TGF-β superfamily member whose signaling requires receptor dimer formation and downstream effectors including Smads, mitogen-activated protein kinases, extracellular signal-regulated kinase, and p38 among others. The effects of activin A signaling are cell context dependent. For example, through interaction with p53, activin A can induce either dorsal or ventral mesoderm formation during *Xenopus* embryogenesis (39), erythroid differentiation (40), or cell cycle arrest through p21 induction and CDK4 downregulation (41).

In breast tumor cell lines, activin A induces growth arrest and inhibits hepatocyte growth factor–induced tubule formation in primary mammary epithelial cells grown in a collagen matrix (32, 42). However, the role of activin A in breast tumorigenesis remains ambiguous. Activin A mRNA and protein are frequently upregulated in DCIS and in IDC compared with normal breast. Moreover, breast tumors with local recurrence or metastasis to lymph nodes have the highest levels of activin A expression (43, 44), highlighting the potential predictive value of activin A as biomarker. Gains in chromosomes 3p, 7p, 12q, and 15q, which contain the genes encoding the activin A type II receptor, activin A, two other activin family members, and Smad 3, are often observed in breast cancer (45–48). Last, activin A overexpression increases tumor volume by inhibiting apoptosis in mouse xenographs (49). This paradox is reminiscent of that described for TGF-β. The induction of growth arrest described here in HMEC (intact p16) and elsewhere (32, 50) supports that activin A acts as a barrier to tumor initiation. In contrast, the observation that activin A is frequently upregulated in IDC and metastatic breast lesions suggests that activin A, such as TGF-β, may facilitate tumorigenesis in the context of impaired growth-inhibitory response (for example, due to loss of p16 in vHMEC) by decreasing immune response and altering the tumor microenvironment. Despite the similarity between activin A and TGF-β, these proteins are not synonymous, since vHMEC arrest in response to TGF-β (4). Inhibiting activin A, either through the induction of physiologic regulators (follistatin, inhibin A, or follistatin-related protein FLRG) or use of inhibitors (SB432542 or type I and II receptor antibodies), is an attractive therapeutic approach to ablate the COX-2 overexpression triggered by DNA damage, although side effects of such therapies remain to be investigated.

DNA damage is an early and nearly universal event in epithelial cancers. It is well appreciated that in the absence of cell cycle checkpoints (e.g., p53 or p16/Rb), DNA damage generates genomic instability and, consequently, may result in random loss of tumor suppressors, gain of oncogenes, and clonal expansion. Thus, DNA damage indirectly contributes to tumorigenesis through the generation of genomic instability. Here, we show that DNA damage may also directly contribute to tumorigenesis through a separate mechanism, the specific induction of activin A and COX-2. Because activin A and the prostaglandins are secreted, DNA damage in one cell could drive tumorigenic phenotypes in an adjacent p16-compromised precursor cell or lead to proliferative arrest in an adjacent p16-intact cell. We postulate that these cell-nonautonomous effects might provide a proliferative advantage to precursor lesions and facilitate the expression of premalignant phenotypes. Understanding how DNA damage contributes to

cell-autonomous and cell-nonautonomous events will further elucidate the tumorigenic process. For example, it may provide novel insights into the ecology of breast tissues and cell-cell interactions that modulate early events in malignancy, identify people with an increased propensity to develop aggressive tumors, or finally, provide an opportunity to prevent the progression of a precursor lesion to a fully tumorigenic state.

Disclosure of Potential Conflicts of Interest

Acknowledgments

Grant Support

References

1. Marnett LJ. The COXIB experience: a look in the rearview mirror. Annu Rev Pharmacol Toxicol 2009;49:265–90.
2. Stack E, DuBois RN. Role of cyclooxygenase inhibitors for the prevention of colorectal cancer. Gastroenterol Clin North Am 2001;30: 1001–10.
3. Crawford YG, Gauthier ML, Joubel A, et al. Histologically normal human mammary epithelia with silenced p16(INK4a) overexpress COX-2, promoting a premalignant program. Cancer Cell 2004;5:263–73.
4. Gauthier ML, Pickering CR, Miller CJ, et al. p38 regulates cyclooxygenase-2 in human mammary epithelial cells and is activated in premalignant tissue. Cancer Res 2005;65:1792–9.
5. Greenhough A, Smartt HJ, Moore AE, et al. The COX-2/PGE2 pathway: key roles in the hallmarks of cancer and adaptation to the tumour microenvironment. Carcinogenesis 2009;30:377–86.
6. Wang D, Dubois RN. Prostaglandins and cancer. Gut 2006;55:115–22.
7. Visscher DW, Pankratz VS, Santisteban M, et al. Association between cyclooxygenase-2 expression in atypical hyperplasia and risk of breast cancer. J Natl Cancer Inst 2008;100:421–7.
8. Yang WT, Lewis MT, Hess K, et al. Decreased TGFβ signaling and increased COX2 expression in high risk women with increased mammographic breast density. Breast Cancer Res Treat. Epub 25 Feb 2009.
9. Gauthier ML, Berman HK, Miller C, et al. Abrogated response to cellular stress identifies DCIS associated with subsequent tumor events and defines basal-like breast tumors. Cancer Cell 2007;12:479–91.
10. Li Z, Schem C, Shi YH, Medina D, Zhang M. Increased COX2 expression enhances tumor-induced osteoclastic lesions in breast cancer bone metastasis. Clin Exp Metastasis 2008;25:389–400.
11. Bos PD, Zhang XH, Nadal C, et al. Genes that mediate breast cancer metastasis to the brain. Nature 2009;459:1005–9.
12. Lucci A, Krishnamurthy S, Singh B, et al. Cyclooxygenase-2 expression in primary breast cancers predicts dissemination of cancer cells to the bone marrow. Breast Cancer Res Treat 2009;117:61–8.
13. Boland GP, Butt IS, Prasad R, Knox WF, Bundred NJ. COX-2 expression is associated with an aggressive phenotype in ductal carcinoma *in situ*. Br J Cancer 2004;90:423–9.
14. Ristimaki A, Sivula A, Lundin J, et al. Prognostic significance of elevated cyclooxygenase-2 expression in breast cancer. Cancer Res 2002;62:632–5.
15. Baron JA, Sandler RS, Bresalier RS, et al. A randomized trial of rofecoxib for the chemoprevention of colorectal adenomas. Gastroenterology 2006;131:1674–82.
16. Bertagnolli MM, Eagle CJ, Zauber AG, et al. Celecoxib for the prevention of sporadic colorectal adenomas. N Engl J Med 2006;355: 873–84.
17. Kwan ML, Habel LA, Slattery ML, Caan B. NSAIDs and breast cancer recurrence in a prospective cohort study. Cancer Causes Control 2007;18:613–20.
18. Thun MJ, Namboodiri MM, Heath CW, Jr. Aspirin use and reduced risk of fatal colon cancer. N Engl J Med 1991;325:1593–6.
19. Dajani EZ, Islam K. Cardiovascular and gastrointestinal toxicity of selective cyclo-oxygenase-2 inhibitors in man. J Physiol Pharmacol 2008;59 Suppl 2:117–33.
20. Romanov SR, Kozakiewicz BK, Holst CR, Stampfer MR, Haupt LM, Tlsty TD. Normal human mammary epithelial cells spontaneously escape senescence and acquire genomic changes. Nature 2001;409: 633–7.
21. Pickering MT, Kowalik TF. Rb inactivation leads to E2F1-mediated DNA double-strand break accumulation. Oncogene 2006;25: 746–55.
22. Tatsumi Y, Sugimoto N, Yugawa T, Narisawa-Saito M, Kiyono T, Fujita M. Deregulation of Cdt1 induces chromosomal damage without rereplication and leads to chromosomal instability. J Cell Sci 2006;119:3128–40.
23. Dumont N, Bakin AV, Arteaga CL. Autocrine transforming growth factor-β signaling mediates Smad-independent motility in human cancer cells. J Biol Chem 2003;278:3275–85.
24. Fordyce CA, Heaphy CM, Griffith JK. Chemiluminescent measurement of telomere DNA content in biopsies. Biotechniques 2002;33: 144–8.
25. Bailey SM, Brenneman MA, Halbrook J, Nickoloff JA, Ullrich RL, Goodwin EH. The kinase activity of DNA-PK is required to protect mammalian telomeres. DNA Repair (Amst) 2004;3:225–33.
26. Karlseder J, Broccoli D, Dai Y, Hardy S, de Lange T. p53- and ATM-dependent apoptosis induced by telomeres lacking TRF2. Science 1999;283:1321–5.
27. Munoz P, Blanco R, Flores JM, Blasco MA. XPF nuclease-dependent telomere loss and increased DNA damage in mice overexpressing TRF2 result in premature aging and cancer. Nat Genet 2005;37: 1063–71.
28. Oh BK, Kim YJ, Park C, Park YN. Up-regulation of telomere-binding proteins, TRF1, TRF2, and TIN2 is related to telomere shortening during human multistep hepatocarcinogenesis. Am J Pathol 2005; 166:73–80.
29. Richter T, Saretzki G, Nelson G, Melcher M, Olijslagers S, von Zglinicki T. TRF2 overexpression diminishes repair of telomeric single-strand

breaks and accelerates telomere shortening in human fibroblasts. Mech Ageing Dev 2007;128:340–5.

30. Cocolakis E, Lemay S, Ali S, Lebrun JJ. The p38 MAPK pathway is required for cell growth inhibition of human breast cancer cells in response to activin. J Biol Chem 2001;276:18430–6.

31. de Guise C, Lacerte A, Rafiei S, et al. Activin inhibits the human Pit-1 gene promoter through the p38 kinase pathway in a Smad-independent manner. Endocrinology 2006;147:4351–62.

32. Burdette JE, Jeruss JS, Kurley SJ, Lee EJ, Woodruff TK. Activin A mediates growth inhibition and cell cycle arrest through Smads in human breast cancer cells. Cancer Res 2005;65:7968–75.

33. de Moraes E, Dar NA, de Moura Gallo CV, Hainaut P. Cross-talks between cyclooxygenase-2 and tumor suppressor protein p53: Balancing life and death during inflammatory stress and carcinogenesis. Int J Cancer 2007;121:929–37.

34. Shim V, Gauthier ML, Sudilovsky D, et al. Cyclooxygenase-2 expression is related to nuclear grade in ductal carcinoma in situ and is increased in its normal adjacent epithelium. Cancer Res 2003;63: 2347–50.

35. Meeker AK, Argani P. Telomere shortening occurs early during breast tumorigenesis: a cause of chromosome destabilization underlying malignant transformation? J Mammary Gland Biol Neoplasia 2004; 9:285–96.

36. Nusing RM, Barsig J. Induction of prostanoid, nitric oxide, and cytokine formation in rat bone marrow derived macrophages by activin A. Br J Pharmacol 1999;127:919–26.

37. Tsatsanis C, Androulidaki A, Venihaki M, Margioris AN. Signalling networks regulating cyclooxygenase-2. Int J Biochem Cell Biol 2006;38:1654–61.

38. Han JA, Kim JI, Ongusaha PP, et al. P53-mediated induction of Cox-2 counteracts p53- or genotoxic stress-induced apoptosis. EMBO J 2002;21:5635–44.

39. Takebayashi-Suzuki K, Funami J, Tokumori D, et al. Interplay between the tumor suppressor p53 and TGF β signaling shapes embryonic body axes in Xenopus. Development 2003;130:3929–39.

40. Sehy DW, Shao LE, Yu AL, Tsai WM, Yu J. Activin A-induced differentiation in K562 cells is associated with a transient hypophosphorylation of RB protein and the concomitant block of cell cycle at G1 phase. J Cell Biochem 1992;50:255–65.

41. Zauberman A, Oren M, Zipori D. Involvement of p21(WAF1/Cip1), CDK4 and Rb in activin A mediated signaling leading to hepatoma cell growth inhibition. Oncogene 1997;15:1705–11.

42. Liu QY, Niranjan B, Gomes P, et al. Inhibitory effects of activin on the growth and morpholgenesis of primary and transformed mammary epithelial cells. Cancer Res 1996;56:1155–63.

43. Mylonas I, Jeschke U, Shabani N, Kuhn C, Friese K, Gerber B. Inhibin/activin subunits (inhibin-α, -βA and -βB) are differentially expressed in human breast cancer and their metastasis. Oncol Rep 2005;13:81–8.

44. Reis FM, Luisi S, Carneiro MM, et al. Activin, inhibin and the human breast. Mol Cell Endocrinol 2004;225:77–82.

45. Sjoblom T, Jones S, Wood LD, et al. The consensus coding sequences of human breast and colorectal cancers. Science 2006; 314:268–74.

46. Bieche I, Khodja A, Driouch K, Lidereau R. Genetic alteration mapping on chromosome 7 in primary breast cancer. Clin Cancer Res 1997;3:1009–16.

47. Bieche I, Lidereau R. Genetic alterations in breast cancer. Genes Chromosomes Cancer 1995;14:227–51.

48. Aubele MM, Cummings MC, Mattis AE, et al. Accumulation of chromosomal imbalances from intraductal proliferative lesions to adjacent in situ and invasive ductal breast cancer. Diagn Mol Pathol 2000;9:14–9.

49. Krneta J, Kroll J, Alves F, et al. Dissociation of angiogenesis and tumorigenesis in follistatin- and activin-expressing tumors. Cancer Res 2006;66:5686–95.

50. Kalkhoven E, Roelen BA, de Winter JP, et al. Resistance to transforming growth factor β and activin due to reduced receptor expression in human breast tumor cell lines. Cell Growth Differ 1995;6: 1151–61.